Flexible operation of CSIRO's post-combustion CO_2 capture pilot plant at the AGL Loy Yang power station

Mai Bui[a], Indra Gunawan[b*], Vincent Verheyen[c], Paul Feron[d], Erik Meuleman[e]

[a]School of Applied Sciences and Engineering, Faculty of Science, Monash University, Victoria, Australia
[b]School of Engineering and Information Technology, Federation University Australia, Churchill 3842, Victoria, Australia
[c]School of Applied and Biomedical Sciences, Federation University Australia, Churchill 3842, Victoria, Australia
[d]CSIRO Energy Flagship - Newcastle, Mayfield West 2304, New South Wales, Australia
[e]CSIRO Energy Flagship - Melbourne, Clayton 3168, Victoria, Australia

* Corresponding author. Tel: +61 3 51226639 Email: indra.gunawan@federation.edu.au

Abstract

Flexible operation has the potential to significantly improve the economic viability of post-combustion CO_2 capture (PCC). However, the impact of disturbances from flexible operation of the PCC process is unclear. The purpose of this study was to investigate the effects of flexible operation in a PCC pilot plant by implementing step-changes for improved dynamic data reliability. The flexible operation campaign was conducted at the CSIRO PCC pilot plant at AGL Loy Yang using monoethanolamine (MEA) absorbent. The pilot plant was operated under a broad range of transient conditions (changing flue gas flow, liquid absorbent flow and steam pressure) to capture the dynamics of a PCC process during flexible operation. The study demonstrated that the dynamics of flue gas flow rate was faster than absorbent flow rate. The greatest CO_2 removal % was achieved at the lowest flue gas flow rate or at the highest absorbent flow rate; however the latter provided improved energy efficiency. The steam pressure parameter could adjust the temperature of all columns simultaneously which can be used to compensate for effects from ambient conditions or heat losses. These results verify the technical feasibility of flexible PCC operation and provide a suitable dataset for dynamic model validation.

Keywords:

Post-combustion CO_2 capture, flexible operation, pilot plant, transient, dynamic modelling

1. Introduction

Greenhouse gas (GHG) emissions have been linked to global warming. Projections indicate that the GHG effect has increased severe environmental impacts including sea level rises, flooding of coastal cities and extreme inland drought (IPCC, 2014). Thus, there is strong motivation to develop low emissions fossil fuel energy via CO_2 capture and storage technologies. Post-combustion CO_2 capture (PCC) plant using amine chemical absorption is the most advanced CO_2 capture technology to date. The first commercial-scale plant at the SaskPower Boundary Dam Power Station in Canada began operation in 2014 (Stéphenne, 2014).

There is a growing interest in implementing flexible operation of PCC plants as modelling studies demonstrate improvements to economic and technical performance (Cohen et al., 2010b; Cohen et al., 2010a; Husebye et al., 2011; Arce et al., 2012; Chen et al., 2012; Cohen et al., 2012; Zhang et al., 2012; Mac Dowell and Shah, 2013; Bui et al., 2014b; van der Wijk et al., 2014; Mac Dowell and Shah, 2015). However, flexible operation imposes process disturbances as the CO_2 capture plant is ramped up, ramped down or turned off and on. The immediate and long-term effect of flexible operation on the process performance of PCC is unclear. Dynamic PCC models will be important tools to clarify the viability of flexible operation and its influence on CO_2 absorption performance (Lawal et al., 2010). However, the validity of dynamic models requires validation against real plant data that demonstrates transient or dynamic behaviour.

Generally, available pilot plant operational data only covers steady state conditions. Thus, most existing dynamic models conducted dynamic model validation with only steady state pilot plant data (Kvamsdal et al., 2009; Lawal et al., 2009b, 2009a; Lawal et al., 2010; Lawal et al., 2012; Bui et al., 2014b). These studies highlighted the need for reliable dynamic pilot plant results to become available. Some studies with access to transient pilot plant data have successfully conducted dynamic validations of dynamic PCC models (Kvamsdal et al., 2010; Biliyok et al., 2012). The transient pilot plant scenario used by Kvamsdal et al. (2010) to validate a dynamic PCC model was one pilot plant run that demonstrated the effects of (i) changing liquid and gas flow rate, and (ii) changing CO_2 content at the gas inlet. In contrast, the dynamic model validation by Biliyok et al. (2012) used the transient pilot plant data for increasing moisture in flue gas and absorber intercooling. Although the dynamic models for both studies were unable to predict absolute values, they provided reasonable predictions of trends.

Hypothetically, the accuracy of dynamic models may improve when validating with dynamic data from multiple pilot plants with different geometry or other operating conditions. To reliably validate further iterations of dynamic PCC models, there is an obvious need for more dynamic pilot plant data to become available (Bui et al., 2014b). Additionally, different process parameters vary in the degree of disturbance magnitude and response time. It should be noted that PCC pilot plants are much smaller in size compared to their commercial-scale counterparts. Dynamic modelling studies estimate the geometry of industrial absorber columns to be ≤12 m in diameter and 17-37 m for packing height (Lawal et al., 2012; Lin et al., 2012; Nittaya et al., 2014). In comparison to commercial-scale, the impact of ambient temperature and heat loss may be amplified for small pilot-scale plants. Additionally, process response times and optimal process control settings will vary from pilot to full scale. Thus, it is important to highlight that data from a pilot-scale plant may not necessarily be optimal in terms of energy requirements and process control.

To capture the entire dynamics of a PCC system, it is important that pilot plant data sets should cover a wide range of flexible operating conditions. Flexible operation data from dynamic PCC pilot plants would provide further practical insight into process performance and ideal operation strategies. Furthermore, dynamic PCC models validated across a broad operating range may have the versatility for applications in modelling flexible PCC operation. Important considerations when designing a pilot plant campaign for collection of reliable results include: (i) minimise the influence of external factors (e.g. ambient temperature fluctuation), (ii) ensure the operation strategy provides reproducible results, and (iii) implement optimised data measurement techniques to ensure data accuracy and validity (particularly for parameters essential for model validation).

The purpose of this study is to investigate the effects of flexible operation in a PCC pilot plant by implementing step-changes to improve the reliability of the dynamic data. The flexible operation campaign is conducted at the CSIRO PCC pilot plant at AGL Loy Yang using monoethanolamine (MEA) absorbent. The step-change approach to plant operation is implemented to minimise the impact of process disturbances and reduce data variability. Also, the pilot plant is operated under a broad range of transient conditions where three control parameters undergo step-changes: (i) flue gas flow rate, (ii) liquid absorbent flow rate, and (iii) steam pressure. These process parameters are suitable for dynamic operation as they provide relatively fast response times and an observable effect on CO_2 capture performance. The objective is to capture the

dynamics of a PCC process during flexible operation and provides a suitable dataset for dynamic model validation.

2. Experimental

2.1 CSIRO PCC Pilot Plant at Loy Yang

The AGL Loy Yang A power station is a 2.21 gigawatt brown-coal fired power station and is located in the Latrobe Valley of Victoria, Australia. The CSIRO PCC pilot plant captures CO_2 from slipstream flue gas. This flue gas is (i) high temperature ranging from 160-180 °C, (ii) high moisture content, and (iii) contains alkaline ash (Cottrell et al., 2008). Additionally, Victorian power plants have electrostatic precipitators to reduce flue gas particulates, but lacks flue gas desulphurisation (FGD) and denitrification (deNO$_X$) (Dave et al., 2011). Table 1 shows the typical flue gas composition of the pilot plant feed coming from the AGL brown coal-fired power plant. These flue gas properties present a challenging process environment for chemical absorption with amine absorbents.

Equation 1: Total volume of absorbent

$$\text{Absorbent Volume (L)} = 123.9 + \text{buffer tank level } \% \times 4.424$$

Table 1: Typical brown coal flue gas composition from the AGL power station, adapted from Artanto et al. (2012).

Flue Gas Component	Composition
H_2O (vol% - wet)	20-23
CO_2 (vol% - wet)	10-11
O_2 (vol% - wet)	4-5
N_2 (vol% - wet)	61-66
SO_2 (wet ppm volume)	120-200
NO_X (wet ppm volume) ~99% NO the balance is NO_2 & N_2O	150-250

The PCC pilot plant was first commissioned in 2008 and is designed to process 50 kg/h of flue gas (Artanto et al., 2012; Artanto et al., 2014). The CSIRO PCC pilot plant is operated during daytime hours. The PCC pilot plant (Figure 1) processes the flue gas in the following sequence: (i) Pre-treatment column, (ii) Absorber Column 2, (iii) Absorber Column 1, and (iv) Stripper Column. The pre-treatment column scrubs the flue gas with sodium hydroxide to remove SO$_X$, NO$_X$ (other than NO) and particulates; thereby minimising amine degradation in the CO_2-absorption process. The liquid absorbent used for CO_2 capture in this study is 30 % (w/w) aqueous monoethanolamine (MEA). The absorbent inventory ranges between 150-250 L which is

calculated by Equation 1. The value 123.9 L represents the total hold-up in the columns, pipes etc. and 4.468 is the volume in litres per level percentage in the buffer tank.

The two absorber columns are operated in series (can also be reconfigured to operate in parallel) and constructed from 200 DN stainless steel pipe. Each absorber column has an inner diameter (ID) of 211 mm, two 1.35 m packed bed sections (i.e. total packing height of 2.7 m), and the total column height is 9.4 m. The single stripper column is constructed from 150 DN stainless steel pipe with 161 mm ID. The stripper is a total column height of 6.9 m and packing height of 3.9 m. The metal random Pall ring packing used in every column has the following general specifications: (i) size/dimensions of 16 mm, (ii) specific area of 338 m^2/m^3, and (iii) packing factor of 306 m^{-1}. The steam for the stripper reboiler is generated by a 120 kW electric boiler (Artanto et al., 2009).

Flow meters, sensors, probes and transmitters installed throughout the CSIRO pilot plant provide instantaneous measurements of flow rate, pressure and temperature. Column temperature profiles can be generated using resistance temperature detectors (RTDs) located along the height of each column. The Gasmet^{TM} FTIR gas analyser also measures gas composition online. Density meters display online density measurements are recorded every minute. During pilot plant operation, liquid absorbent samples are titrated onsite to monitor MEA concentration. If necessary, operators will adjust concentration to meet the required concentration of MEA 30 % (w/w). Once the pilot plant reaches steady state operation (times provided in Table 6), absorbent is sampled at various points in the pilot plant and sent off-site for liquid analysis. The concentration of CO_2 and MEA is determined with an automatic titrator (Artanto et al., 2012). The liquid analysis results are presented as w/w% concentration of CO_2 and MEA, CO_2 loading and density.

2.2 Experimental Program: Step-change Approach for Dynamic Operation

The lack of published dynamic pilot plant data may be attributed to most PCC pilot plants not being equipped for online measurements of liquid composition (i.e. CO_2 concentration, CO_2 loading). Subsequently, knowledge and experience about dynamic pilot plant operation is limited. All pilot plants will undergo "dynamic" operation at some point, for example start-up or shut down. However, the transient behaviour during such large disturbances is highly variable and difficult to reproduce (Bui et al., 2014a). Additionally, in the case of outdoor pilot plants that treat real flue gas, measurements are influenced by external factors such as (i) weather or ambient temperature affecting columns, pipelines and cooling water, (ii) temperature change of flue gas from the power station, and (iii) change in flue gas composition. These external factors

introduce further variability to pilot plant results, and hence need to be monitored. The CSIRO PCC pilot plant in Loy Yang is suited for dynamic operation research due to its relatively small scale with fast dynamics, temperature indicators and the presence of density meters which can provide real-time estimates of liquid phase CO_2 concentration and CO_2 loading. Additionally, thermal insulation on the steel piping, absorber columns and stripper column minimises the influence of ambient temperature.

The "step-change" operation approach has been developed for this dynamic pilot plant study to address variability issues. Inspiration for the step-change techniques came from Gruber (2004) who used a steady state "snapshots" approach to modelling dynamic behaviour. Originally, Gruber (2004) developed this technique as a means of modelling dynamic systems using a steady state process simulation software. Incremental changes were made to the process and the steady state solutions simulated. These steady state "snapshots" in time could be plotted together to provide the overall dynamic solution (Gruber, 2004). In this study, the same approach is applied to dynamic operation of a pilot plant with key parameter changes being incremental. The step-change approach has the advantage of minimising disturbances on the process. The application of the step-change technique to pilot plant operation will significantly improve the consistency and reproducibility of dynamic results. This step-wise technique was previously performed in another PCC pilot plants at Esbjerg Power Station in Denmark (Faber et al., 2010) and RWE Power in Germany (Moser et al., 2011).

Before implementing any step-changes, the pilot plant is operated at initial conditions until the process reaches steady state or equilibrium. Generally, the process is considered steady state when CO_2 removal is constant and online measurements for column temperatures and levels are approximately constant. The step-change approach to pilot plant operation involves sequential incremental changes to one set-point parameter (e.g. flue gas or absorbent flows). The successive changes gradually increase or decrease the magnitude of a set-point parameter. Upon making each change, the pilot plant is allowed to run until the process regains conditions of stable conditions and continues to run until an adequate period of steady state data is logged. Most of the condition measurements are instantaneous but sampling of liquids for analysis only occurred during steady state.

The three control parameters that were used to implement the step-change approach included: (i) flue gas flow, (ii) absorbent flow, and (iii) steam pressure. Table 2 identifies the most stable operation range for these control parameters and the range used during the dynamic step-change approach. Some step-changes for

6

flue gas flow and absorbent flow were outside the range for stable operation. The flue gas flow and absorbent flow directly influenced absorption performance. The steam pressure directly manipulated stripper column temperature which controlled the desorption efficiency. The steam pressure had no effect on process stability and was only limited at the maximum range to prevent boiling of amine solution.

Table 2: Parameter range for stable operation of the CSIRO pilot plant at Loy Yang Power and the actual operating range used for the dynamic step-change approach.

	Stable operation	Dynamic step-changes
Flue gas flow (kg/h)	100 – 120	60 – 120
Liquid absorbent flow (L/min)	5.5 – 7.0	5.5 – 7.5
L/G Ratio (L/Nm^3)	3.6 – 4.3	3.6 – 7.1
Steam pressure (kPag)	>120	110 – 170

2.3 Data Required for Dynamic Model Validation

Based on previous dynamic modelling studies, important operational data that has been used in dynamic model validation includes: (i) temperature profiles of the absorber and stripper columns, (ii) measurements of liquid CO_2 loading at various locations in the pilot plant (Kvamsdal et al., 2009; Lawal et al., 2009b, 2009a; Lawal et al., 2010; Lawal et al., 2012), (iii) change in CO_2 captured % with time (Kvamsdal et al., 2010), (iv) CO_2 concentration in the treated flue gas stream, and (v) reboiler heat duty (Biliyok et al., 2012). Thus, this paper presents these important pilot plant results for step-changes of the following operational parameters: flue gas flow, absorbent flow rate, and steam pressure. For effective validation of dynamic PCC models, Appendix B provides detailed data of step-changes in the pilot plant.

2.4 Gas and Liquid Analysis Methods

A Gasmet^{TM} continuous emission monitoring (CEM) system is installed at the CSIRO PCC pilot plant. The gas analysis system uses a Fourier Transform Infra-Red (FT-IR) spectrometer to simultaneously detect 20 components in the gas phase. Oxygen (O_2) composition in gas samples is measured with a built-in ZrO_2 cell analyser. Flue gas properties are measured successively through 5 locations within the pilot plant (shown as G1 to G5 in Figure 1), also ambient samples near the pilot plant are analysed. Three gas samples are collected consecutively at each location to ensure consistency, the first sample flushes the line for one minute and the second two samples are analysed.

During pilot plant operation, MEA concentration is manually monitored onsite and adjusted to maintain at 30% (w/w). Small MEA liquid samples are periodically collected and titrated at the pilot plant. A 1 mL MEA

sample is prepared for titration by first diluting it with water and HCl is added in excess to enable the release of bound CO_2. This solution is then titrated against NaOH to determine the amount of HCl in excess, which in turn can give the amount of HCl consumed by the bound CO_2 via Equation 2. Subsequently, the concentration of MEA can be calculated using Equation 3. If the MEA concentration is not 30% (w/w), this value is restored via the addition or extraction of water. Once pilot plant operation reaches steady state, liquid is sampled from pilot plant locations L1 to L4 in Figure 1. Liquid samples are delivered to CSIRO Clayton laboratories for liquid analysis to measure CO_2 concentration, density, concentrations of total and free MEA, and CO_2 loading.

Equation 2: Moles of MEA (equivalent to the moles of HCl consumed by bound CO_2)

$$n_{MEA} = n_{HCl \text{ initial}} - n_{HCl \text{ excess}} = n_{HCl \text{ initial}} - n_{NaOH \text{ titrated}}$$

Equation 3: Concentration of MEA % (w/w)

$$MEA \% (w/w) = \frac{(n_{HCl \text{ initial}} - n_{NaOH \text{ titrated}}) \times M_W(MEA)}{m(sample)} \times 100$$

2.5 Online CO_2 Concentration Measurements

Conventionally, most pilot plant studies will measure liquid phase CO_2 loading, density and MEA concentration using off-line laboratory analysis (Dugas, 2006; Artanto et al., 2009; Seibert et al., 2010; Simon et al., 2011; Artanto et al., 2012). However, such techniques are unable to illustrate dynamic changes in liquid absorbent composition (van der Ham et al., 2014; van Eckeveld et al., 2014). A few pilot plants have successfully implemented real-time liquid analysis techniques, these include:

1) The National Carbon Capture Centre (NCCC) PCC pilot plant (Wilsonville, Alabama, USA): uses an automatic titration system to determine absorbent concentration and CO_2 loading (Gayheart et al., 2012);

2) The Separations Research Program (SRP) PCC pilot plant (Austin, Texas, USA): determines online CO_2 concentration based on liquid absorbent density and temperature measured by advanced Coriolis mass flow meters (Seibert et al., 2010) – similar approach is used for this present study.

For dynamic pilot plant campaigns, the ability to monitor transient behaviour in the liquid phase is critical. Furthermore, online measurements of liquid phase composition can proactively improve plant process control and hence performance (Seibert et al., 2010; Bui et al., 2014a).

Recent MEA absorbent sensitivity studies demonstrate that liquid phase CO_2 concentration has the strongest correlation with liquid density. However, liquid density has very low correlation with any the concentration of any other tested liquid components (e.g. MEA, HNO_3, H_2SO_4, HEAI, pollutants or temperature) (van der Ham et al., 2014; van Eckeveld et al., 2014). Subsequently, CSIRO installed density meters in their PCC pilot plant so that operators could observe immediate CO_2 composition changes in the absorbent and execute process control appropriately. There are three Endress & Hauser density meters installed in the CSIRO PCC pilot plant at various locations (shown in Figure 1):

D1) ABS-DE01 – Feed lean absorbent into Absorber Column 1;

D2) STR-DE01 – Lean absorbent exiting the Stripper Column;

D3) ABS-DE03 – Rich absorbent at the base of Absorber Column 2.

As illustrated by Figure 1, density meters have been positioned adjacent to absorbent sampling points to enable direct comparison of density meter measurements against results from off-site laboratory analysis.
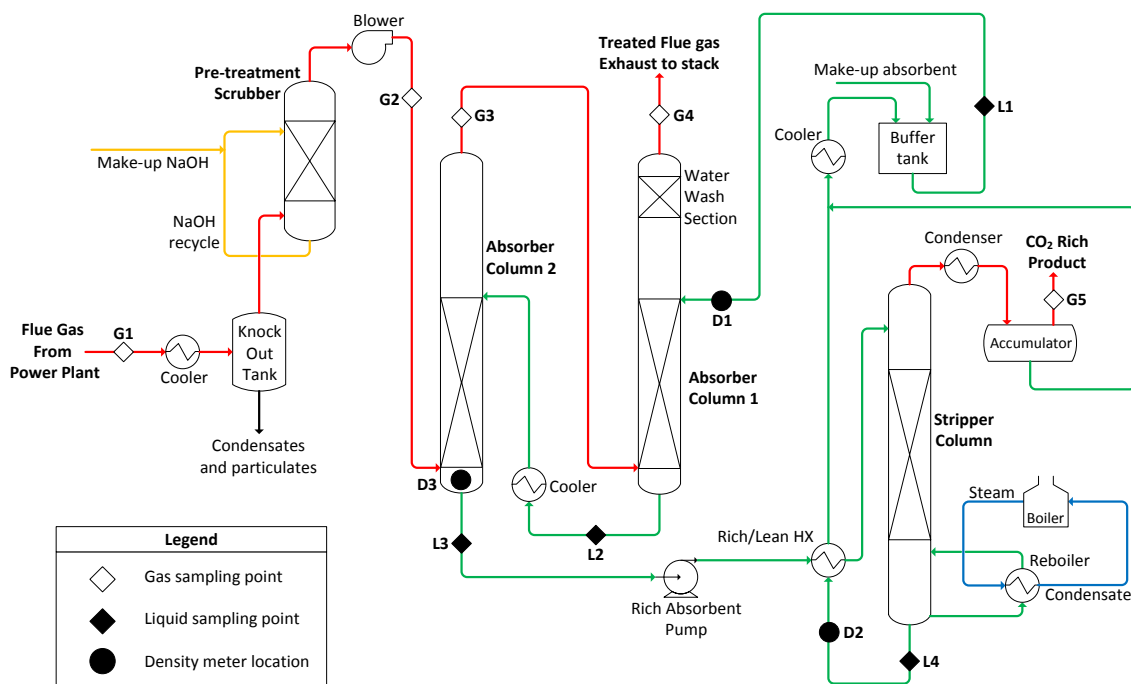

Figure 1: Flow diagram of the CSIRO PCC pilot plant in the AGL Loy Yang power station, Victoria, Australia.

The D2 and D3 density meters have been calibrated against relevant liquid analyses to accurately predict CO_2 concentration in a liquid absorbent. The following density correlations determined for this study are unique to the type of absorbent and pilot plant specifications:

Equation 4: Density correlation to predict CO₂ concentration based on online density measurements for rich absorbent at the base of <mark>A</mark>bsorber <mark>C</mark>olumn 2 (sampling point L3 and meter D3).

$$CO_2 \text{ concentration \% (w/w)} = 48.30206\,\rho - 44.01507$$

Equation 5: Density correlation to predict CO₂ concentration based on online density measurements for lean absorbent exiting the <mark>S</mark>tripper <mark>C</mark>olumn (sampling point L4 and meter D2).

$$CO_2 \text{ concentration \% (w/w)} = 25.16693\,\rho - 20.99081$$

2.6 CO₂ Removal %

The CO_2 removal is calculated based on the concentration of CO_2 in the flue gas as measured at the feed flue gas entering <mark>A</mark>bsorber <mark>C</mark>olumn 2 (sampling point G2) and treated flue gas exiting <mark>A</mark>bsorber <mark>C</mark>olumn 1 (sampling point G4). The CO_2 removal in Equation 6 represents the proportion of CO_2 absorbed from the feed flue gas and is typically equivalent to CO_2 captured. This online CO_2 removal % has been used to demonstrate the transient behaviour during step-change runs.

Equation 6: CO₂ Removal % calculation

$$CO_2 \text{ Removal \%} = \frac{(CO_2 \text{ Mass flow into ABS2}) - (CO_2 \text{ Mass flow exiting ABS1 in treated flue gas})}{(CO_2 \text{ Mass flow into } ABS2)} \times 100$$

2.7 Reboiler Duty for Absorbent Regeneration

Reboiler heat duty and absorbent regeneration energy is expressed as energy per unit of time or energy per amount of CO_2 absorbed. There are two approaches to determine reboiler heat duty required for absorbent regeneration:

1) **Actual reboiler heat duty** is determined from pilot plant measurements for flow of condensed steam and pressure of the steam supplied to the reboiler. However, this value is not truly representative of absorbent regeneration energy due effects from external factors (e.g. fluctuating ambient temperature and heat losses via non-insulated pipes and equipment). Thus, actual reboiler heat duty has not been used in subsequent calculations of reboiler duty for absorbent regeneration.

2) **Calculated reboiler heat duty** for absorbent regeneration ($Q_{reboiler}$) is the combination of three components: (i) CO_2 desorption energy, $Q_{desorption}$; (ii) sensible heat that brings the absorbent to reboiler temperature, $Q_{sensible}$; and (iii) heat required for water evaporation which is equivalent to latent heat of water condensation at the condenser, $Q_{condenser}$. The equations for calculations of absorbent regeneration energy are detailed in Artanto et al. (2012) and Cousins et al. (2012).

3. Results and Discussion

3.1 Effect of Step-changes in Flue Gas Flow Rate
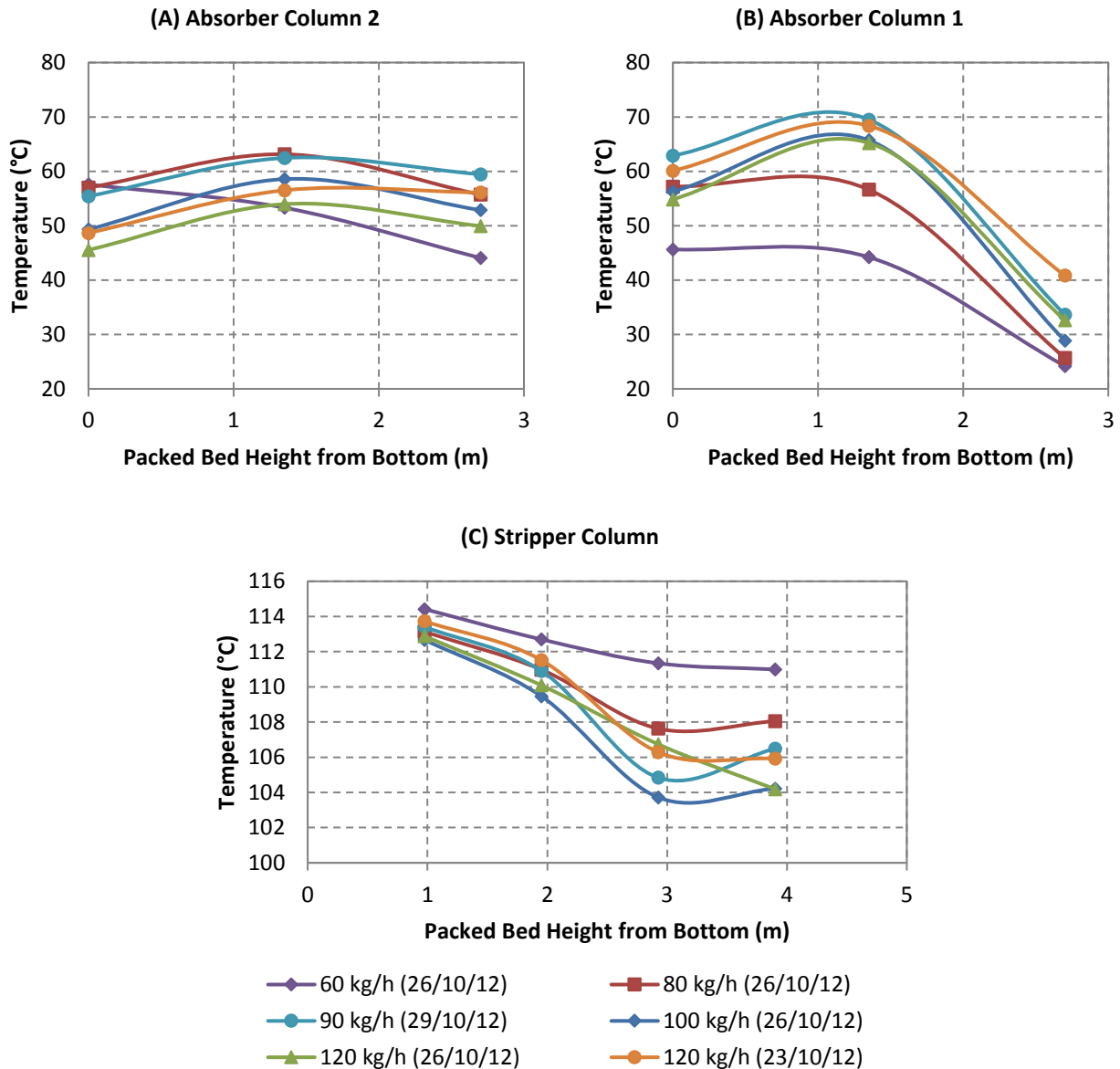
3.1.1 Column Temperature Profiles

Figure 2: Temperature profiles for (A) Absorber Column 2, (B) Absorber Column 1, and (C) the Stripper Column revealing their temperature response due to step-changes in flue gas flow. The operating set point conditions are absorbent flow rate of 5.5 L/min and steam pressure 140 kPag.

The influence of flue gas flow step-changes on column liquid temperature is visualised as changes to the

shape and position of the profiles in Figure 2. In the dual absorber configuration, the feed flue gas entering

ABS2 (18-35 °C) is significantly lower in temperature compared to the inflowing absorbent stream (40-65 °C).

In contrast, the incoming flue gas for ABS1 (45-60 °C) is higher temperature compared to the entering

absorbent stream (39-40 °C). Subsequently as flue gas flow increases, the ABS2 temperature profile shifts down to lower temperatures. Conversely, the ABS1 temperature profile shifts up to higher temperatures. The temperature of the rich absorbent stream exiting ABS2 will directly influence the temperature of the stripper column. This rich absorbent stream is counter-currently heated in the rich/lean cross-heat exchanger by the lean absorbent from the stripper (114-115 °C) where temperature is dependent on reboiler conditions. The overall effect of increasing flue gas flow rate can be summarised as the: (i) cooling of ABS2 and (ii) heating of ABS1, leading to (iii) the cooling of the stripper.

In Figure 2, there are two sets of temperature profiles for flue gas flow rate 120 kg/h from different days. The temperature profiles for 23/10/12 correspond to the day with greater ambient temperature (25.6 °C); these profiles are at higher temperatures compared to those for 26/10/12 (ambient temperature 16.9 °C). Thus, significant changes in ambient temperature can produce an observable effect on pilot plant results. This theory can be confirmed by Appendix C, which illustrates that under constant process conditions, increased ambient temperature generally shifts the column temperature profiles higher.

As amine solutions degrade, significant changes occur in their physical properties, with increases to viscosity, as well as greater susceptibility to foaming and fouling (Lepaumier et al., 2008; Islam et al., 2011). Such property changes were apparent during Dynamic Campaign 1 since aged and degraded MEA absorbent was deliberately being evaluated. Due to the higher viscosity of the aged MEA, liquid distribution was unstable at higher flue gas (≥120 kg/h). The stripper liquid level was particularly difficult to stabilise at high flue gas flow rates. On the other hand, low flue gas flow rate (60 kg/h) enhanced cooling and the feed flue gas enters ABS2 at very low temperatures (~ 18 °C). Thus at flue gas flow 60 kg/h, there was a greater degree of CO_2 absorption at the bottom of ABS2 and significantly high temperatures were observed. Subsequently, inconsistent temperature trends were apparent at the highest and lowest flue gas flow rates of 120 kg/h and 60 kg/h respectively.

3.1.2 CO_2 Removal %, CO_2 Concentration and Reboiler Heat Duty

At constant absorbent flow rate, increases to flue gas flow rate will decrease the liquid to gas ratio (L/G). Furthermore, feed CO_2 entering the absorber becomes excess relative to the absorbent flow and the concentration gradient drives the mass transfer of CO_2 into the liquid phase (forming amine carbamate). Subsequently at higher flue gas flow rates, the carbamate concentration in the absorption section increases as seen in Figure 3 (A). However, increased flue gas flow rate reduces the degree of CO_2 absorption due to

decreased contact time between the liquid and gas phases. Table 3 shows that increased flue gas flow rate reduces CO_2 removal % when the absorbent flow rate is constant (less contact time between the flue gas and absorbent). In contrast, decreasing flue gas flow rate in the absorber (Figure 4) increases the L/G ratio and contact time between the liquid and gas phases for greater CO_2 transfer. The decrease of feed flue gas flow into the absorber reduces the CO_2 concentration gradient which is observed as a decline in liquid CO_2 concentration.

The flue gas flow rate into the absorber columns will influence the performance of the desorption section. Table 3 provides typical reboiler heat duty values calculated for various flue gas flow rates in the pilot plant. Although decreased flue gas flow rate recovers a greater proportion of CO_2 (higher removal %), reboiler heat duty for absorbent regeneration increases (in terms of MJ per kg CO_2). Conversely, CO_2 removal % would decrease as flue gas flow increases, reducing reboiler energy requirements. The reboiler heat duty is composed of three components, $Q_{desorption}$, $Q_{sensible}$ and $Q_{condenser}$. If the absorbent and water flow rates remain constant, increasing flue gas flow rate reduces the temperature in the stripper column (refer to the temperature profiles) and subsequently decreases both $Q_{sensible}$ and $Q_{condenser}$. In contrast, the heat of CO_2 desorption ($Q_{desorption}$) remains constant at 1.9 MJ/kg CO_2 for all flue gas flow rates. Figure 3 (B) shows that the lean absorbent exiting the stripper maintains constant CO_2 concentration across different flue gas flows; indicating the degree of absorbent regeneration remains consistent.
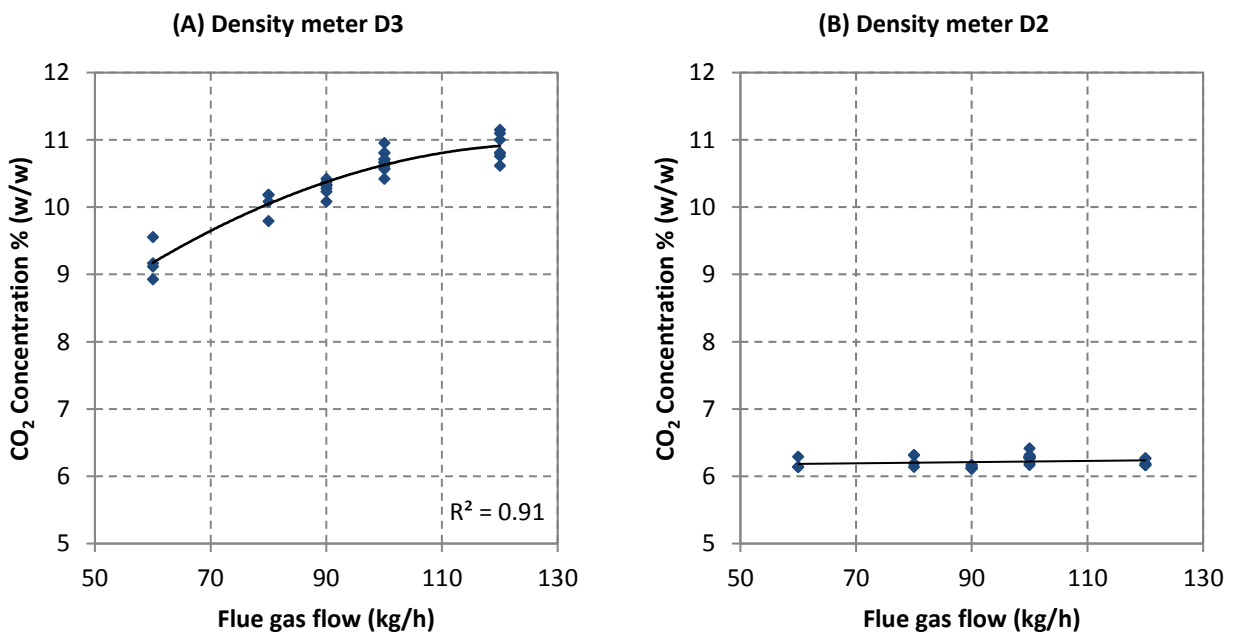

Figure 3: Predicted CO_2 concentration for various flue gas flow rates at (A) density meter D3 and (B) density meter D2. The set point conditions as per Figure 2.
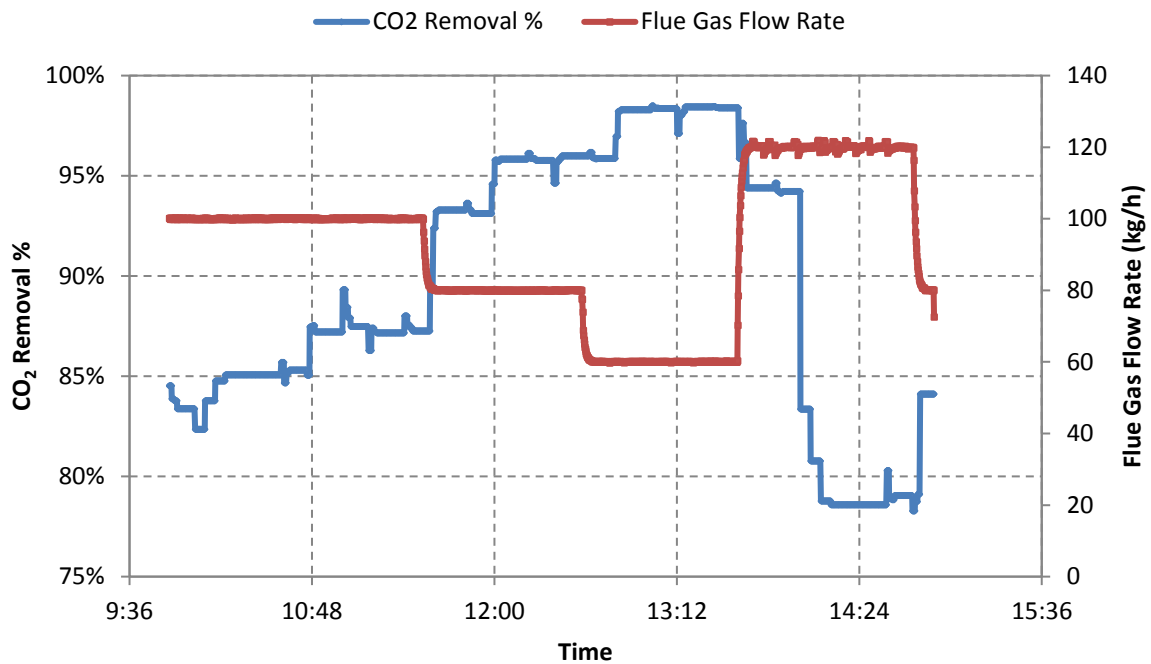
Figure 4: Change in CO$_2$ removal % (proportion of CO$_2$ absorbed from the feed flue gas) during step-changes to flue gas flow rate. The operating set point conditions as per Figure 2.

Table 3: Average CO$_2$ removal % (based on the gas analysis) and reboiler heat duty for different flue gas flow rates at the CSIRO PCC pilot plant. The set point conditions as per Figure 2.

Flue gas flow rate (kg/h)	L/G Ratio (L/Nm³)	Average CO$_2$ Removal %	Reboiler heat duty (MJ/kg CO$_2$)
60	7.09	98	7.8
80	5.32	95	7.0
90	4.73	92	6.3
100	4.26	87	5.9
120 (23/10/12)	3.55	80	5.8
120 (26/10/12)	3.55	82	5.5

3.2 Effect of Step-change in Absorbent Flow Rate
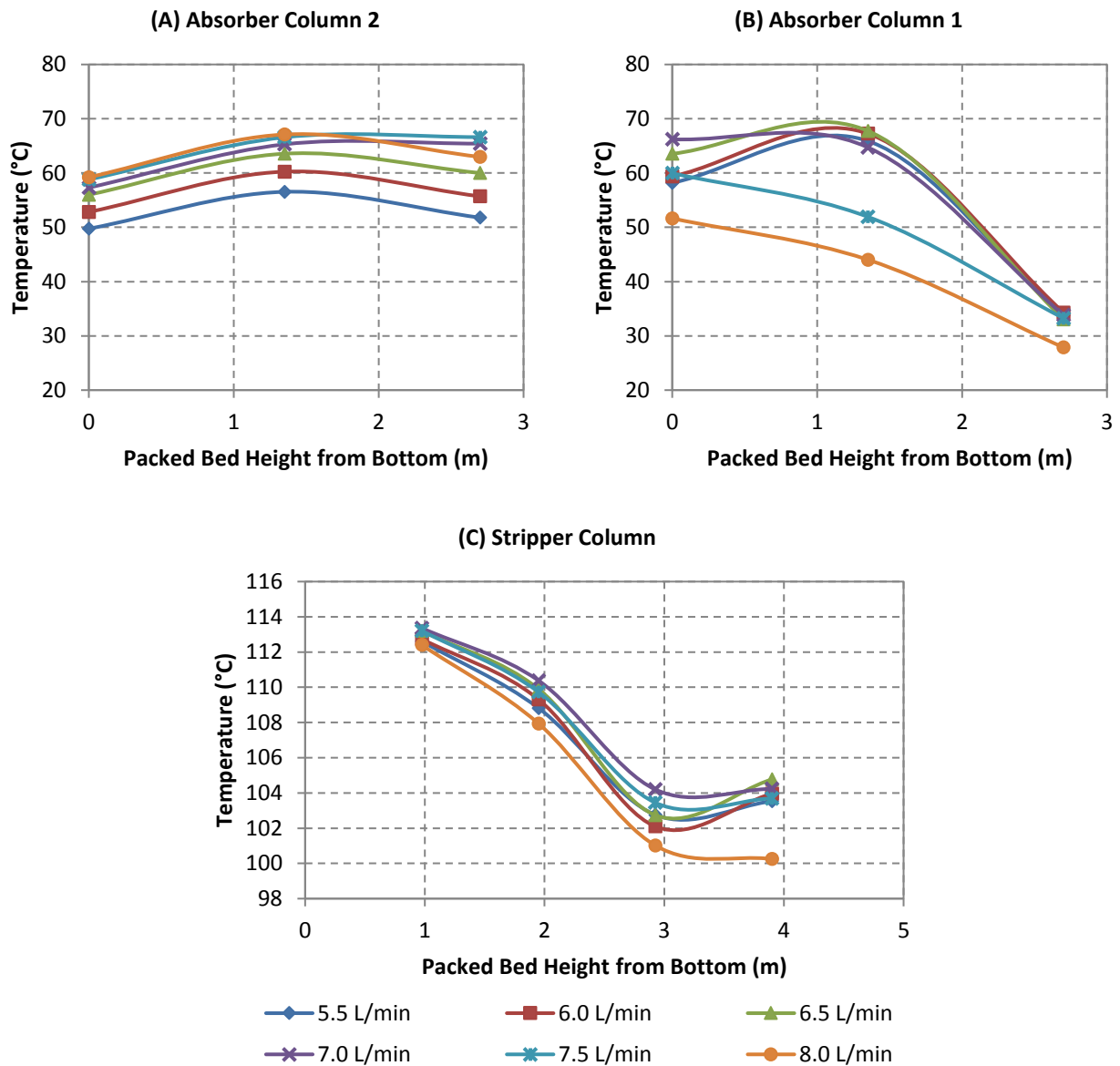
3.2.1 Column Temperature Profiles

Figure 5: Column temperature profiles for (A) Absorber Column 2, (B) Absorber Column 1, and (C) Stripper Column showing step-change in absorbent flow. The operating set point conditions are flue gas flow rate of 100 kg/h and steam pressure 140 kPag.

The temperature profiles for step-changes to absorbent flow rate are illustrated in Figure 5. In the series configuration, the feed absorbent entering ABS2 is at a higher temperature than the flue gas. Hence, increasing step-changes to absorbent flow rate will shift the ABS2 temperature profile to higher temperatures. On the other hand, the absorbent entering ABS1 is at a lower temperature than the inflowing flue gas stream. Thus, the ABS1 temperature profile shifts to lower temperatures when absorbent flow rate is increased. The increase of absorbent flow rate from 5.5 to 7 L/min raises the ABS2 temperature and stripper

temperature ==increases. As absorbent flow rate increases above 7 L/min, the small increase of ABS2 temperature has no influence on the stripper and the stripper temperature decreases due to endothermic CO_2 desorption.== The general behaviour in the series pilot plant configuration during increases to absorbent flow rate is (i) heating of ABS2, (ii) cooling of ABS1, ==as well as== (iii) heating ==and then cooling== of ==the== stripper (converse to behaviour observed during increases to flue gas flow rate). The stability of liquid distribution was difficult to maintain at high absorbent flow rates (≥7 L/min) as a consequence of the higher viscosity of degraded MEA solution. Thus, the temperature profiles at absorbent flow rate 7 L/min or greater were inconsistent with typical behaviour.

3.2.2 CO_2 Removal %, CO_2 Concentration and Reboiler Heat Duty

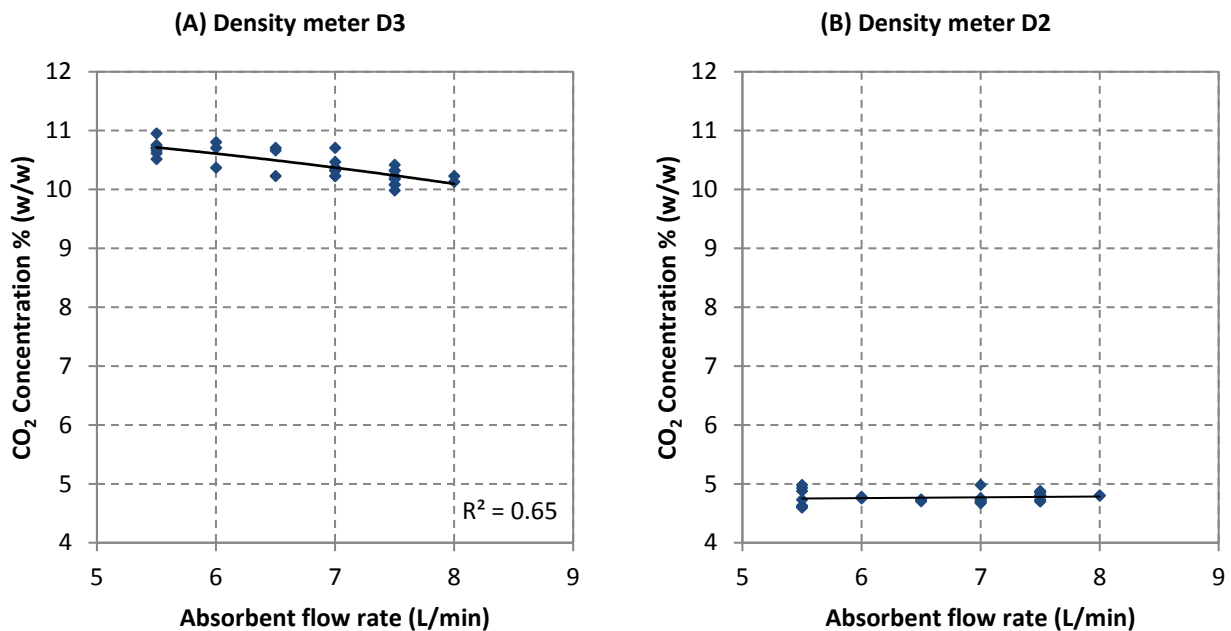**(A) Density meter D3**   **(B) Density meter D2**

Figure 6: Predicted CO_2 concentration for various absorbent flow rates at (A) density meter D3 and (B) density meter D2. The set point conditions are flue gas flow rate 100 kg/h and steam pressure 140 kPag.

Table 4: Average CO_2 removal % (based on the gas analysis) and reboiler heat duty for different absorbent flow rates. The set point conditions as per Figure 5.

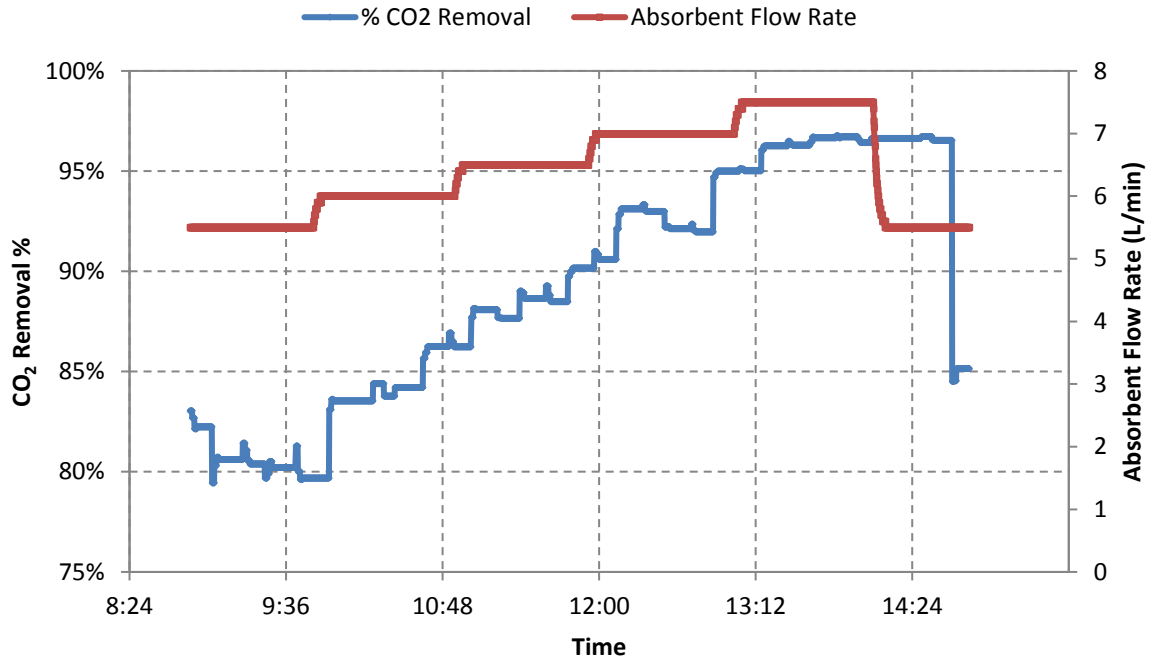| Absorbent flow rate (L/min)	L/G Ratio (L/Nm³)	Average CO_2 Removal %	Reboiler heat duty (MJ/kg CO_2)
5.5	4.26	83	5.8
6.0	4.65	86	5.9
6.5	5.03	92	5.9
7.0	5.42	94	5.7
7.5	5.81	98	5.5
8.0	6.19	98	5.4

Figure 7: Change in CO_2 removal (proportion of CO_2 absorbed from the feed flue gas) during step-changes to absorbent flow rate (proportion of CO_2 recovered from the feed flue gas as stripper CO_2 product). The set point conditions as per Figure 5.
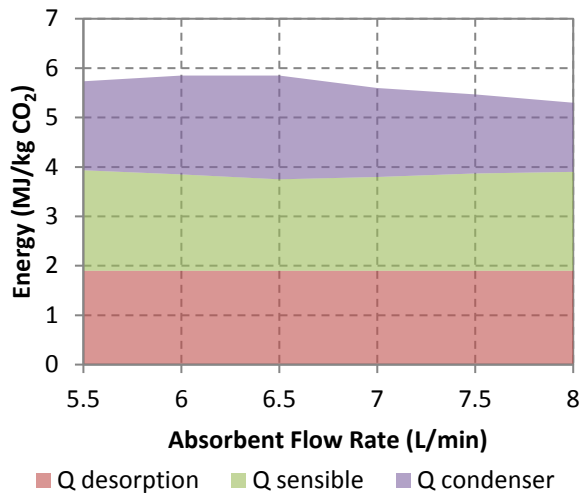

Figure 8: Reboiler heat duty divided into the three components of desorption energy $Q_{desorption}$, $Q_{sensible}$ and $Q_{condenser}$ at various absorbent flow rates.

At high absorbent flow rate, the MEA feed into the absorber is in excess compared to the inflow of CO_2 in the feed flue gas. Thus, the lower CO_2 concentration gradient reduces the mass transfer of CO_2 into the liquid phase. Therefore, CO_2 concentration of the absorbent at the base of the absorber column decreases as absorbent flow rate increases, as demonstrated by Figure 6 (A). In contrast, Figure 7 demonstrates greater CO_2 removal % with increases in absorbent flow rate since more MEA is available to absorb CO_2 from flue gas. As discussed in section 3.4.1, upon introducing a step-change to absorbent flow rate, there is a small

time delay before changes in CO_2 removal % are detected. Furthermore, increases to absorbent flow rate correspond to higher L/G ratio (Table 4). In the stripper section, Figure 6 (B) shows that absorbent flow rate has no influence on constant residual CO_2 concentration in the exiting lean absorbent (location D2). This confirms that sufficient energy was supplied to bring the reboiler up to the required temperature for adequate carbamate breakdown.

The overall effect of absorbent flow rate variation on reboiler heat duty is shown in Table 4. Analysis of the three energy components that formulate reboiler heat duty (Figure 8) provides insight into the behaviour during changes to absorbent flow rate. Over the range of absorbent flow rates, $Q_{desorption}$ remains constant at 1.9 MJ/kg CO_2 (similar behaviour observed during flue gas flow changes). There are competing effects of $Q_{sensible}$ and $Q_{condenser}$ on reboiler heat duty during variations to absorbent flow. The dual effect of increasing absorbent flow rate on the $Q_{sensible}$ formula includes: (i) higher $Q_{sensible}$ due to greater absorbent flow rate; and (ii) lower $Q_{sensible}$ due to greater temperature of the rich absorbent from ABS2. Lastly, $Q_{condenser}$ is dependent on the temperature and flow rate of the cooling water. The cooling water temperature varied between runs due to the influence of ambient temperature. The cooling water flow rate was based on cooling requirements and was adjusted between 75-90 L/min. The overall influence of absorbent flow rate on reboiler heat duty was dependent on which energy component effect dominated (i.e. $Q_{sensible}$ or $Q_{condenser}$).

3.3 Effect of Step-change in Steam Pressure
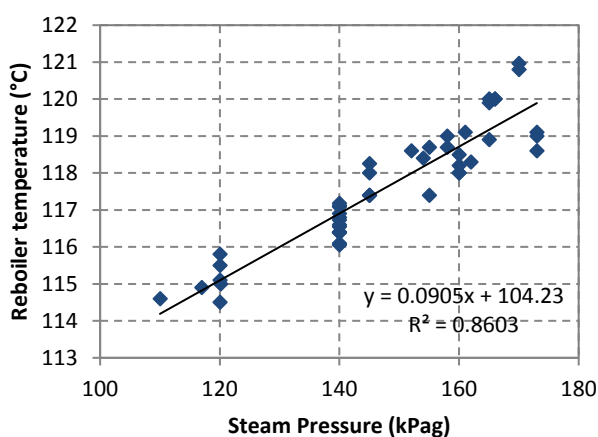
3.3.1 Column Temperature Profiles

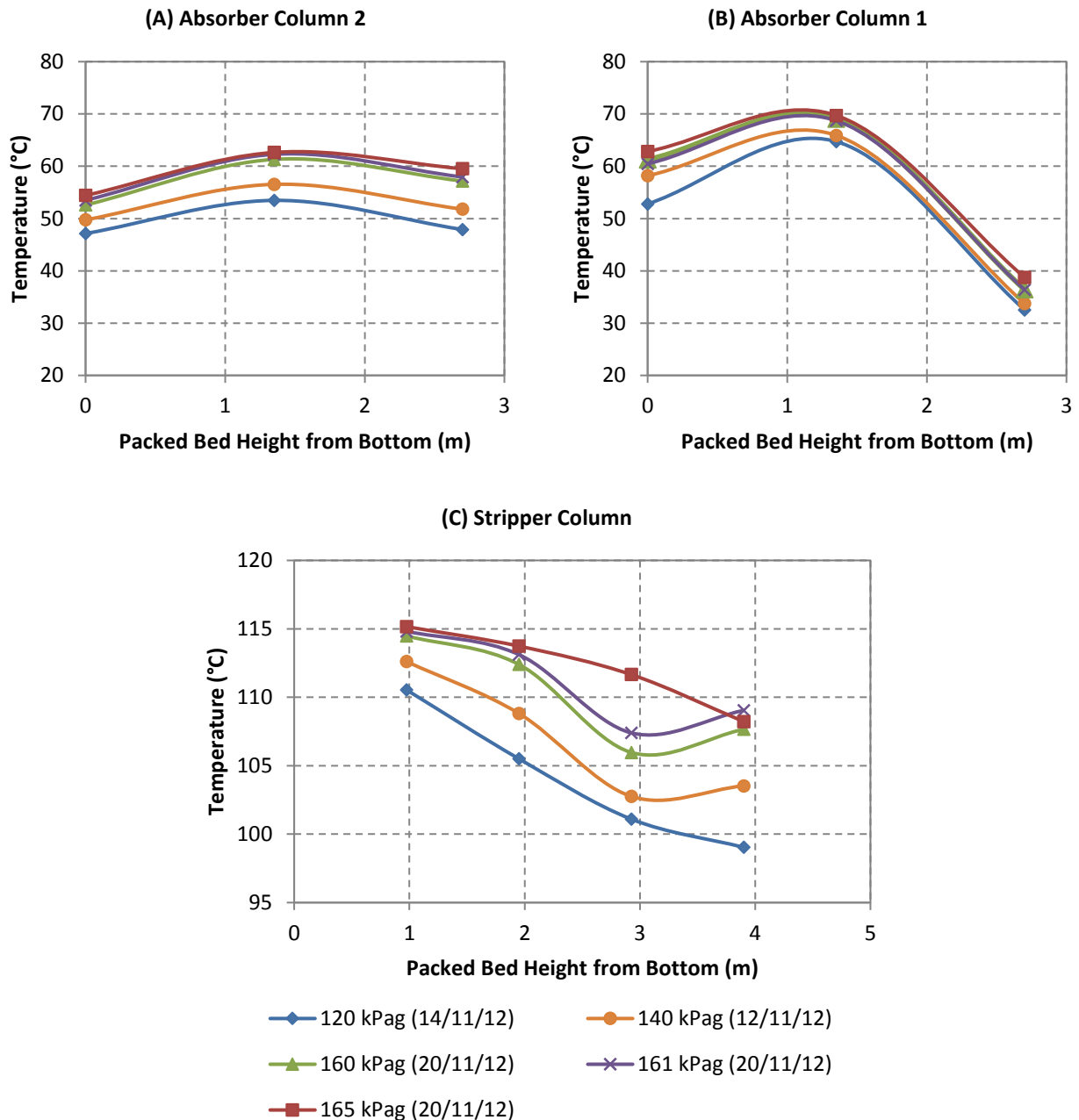Figure 9: The correlation between steam pressure and reboiler temperature.

Figure 10: Column temperature profiles for (A) Absorber Column 2, (B) Absorber Column 1, and (C) Stripper Column showing step-change in steam pressure. The operating set point conditions are flue gas flow rate of 100 kg/h and absorbent flow rate of 5.5 L/min.

Steam pressure is used to control the reboiler temperature in the pilot plant. Figure 9 shows the variation in reboiler temperature with different steam pressures. Despite the presence of thermal insulation, deviations in the Figure 9 correlation indicate the influence of ambient temperature and heat loss. The behaviour of column temperature profiles during steam pressure changes has been illustrated in Figure 10. As the steam pressure is increased, the column temperature profiles shift to higher temperatures for the two absorber and stripper columns. An increase in reboiler temperature subsequently leads to greater lean absorbent

temperature and higher temperature in the absorber section. The shape of the absorber column temperature profiles for both ABS2 and ABS1 are consistent across the range of steam pressures. At steam pressures of 120 kPag and 165 kPag, the liquid level near the top bed of the stripper fluctuates considerably. Subsequently, temperature measured at the top of the packed bed fluctuates causing inconsistencies in the stripper temperature profiles. The increase in steam pressure at the stripper section leads to an overall temperature increase for every column. Thus, the steam pressure parameter may be used for simultaneous temperature adjustment in the whole system. Furthermore, such a capability could be used to compensate for temperature variations that arise due to ambient effects or heat loss.

3.3.2 CO_2 Removal %, CO_2 Concentration and Reboiler Heat Duty
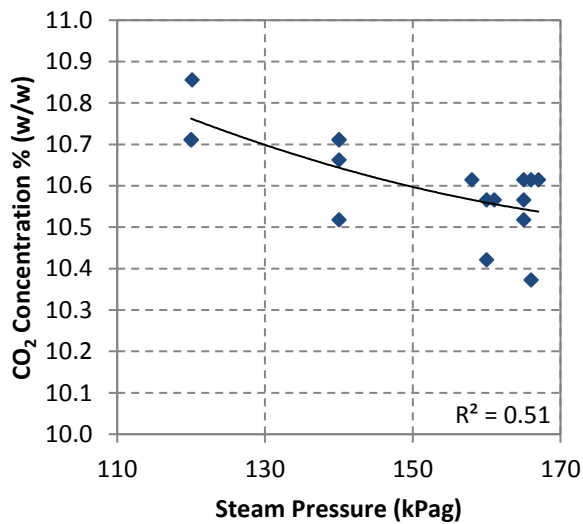
Figure 11: Predicted CO_2 concentration for various steam pressures at density meter D3. The set point conditions as per Figure10.

Table 5: Average CO_2 removal (based on the gas analysis) and reboiler heat duty for different steam pressures at the CSIRO PCC pilot plant. The set point conditions as per Figure 10.

Steam Pressure (kPag)	L/G Ratio (L/Nm³)	Average CO_2 Removal %	Reboiler Heat Duty (MJ/kg CO_2)
120	4.26	71	5.3
140	4.26	80	5.8
160	4.26	89	6.6
161	4.26	92	7.2
165	4.26	93	7.4

Figure 12: Change in CO_2 removal (proportion of CO_2 absorbed from the feed flue gas) during step-changes to steam pressure. The operating set point conditions as per Figure 10.
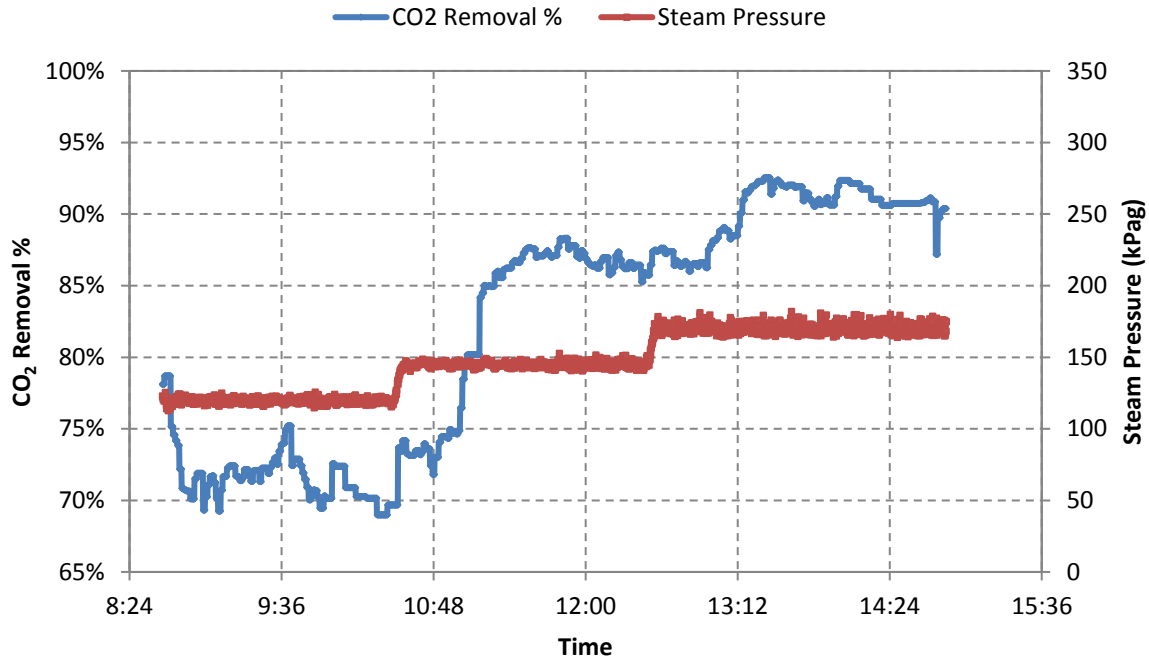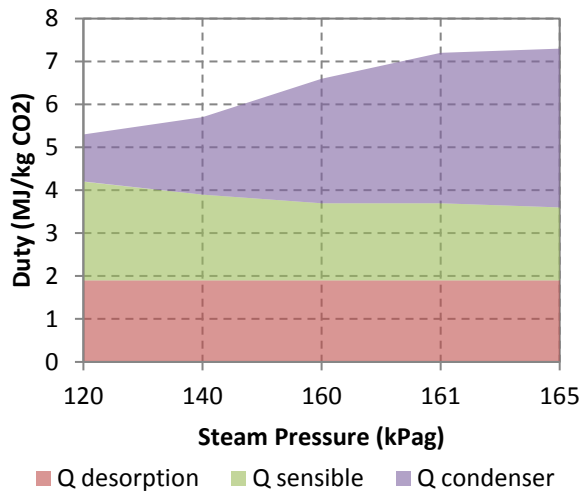

Figure 13: Reboiler heat duty divided into the three components of desorption energy $Q_{desorption}$, $Q_{sensible}$ and $Q_{condenser}$ at various steam pressures.

Density meter measurements at D2 were unavailable for this period of time, thus CO_2 concentration for the lean absorbent is not shown. As mentioned previously, increasing the steam pressure will lead to higher temperatures in the absorber and stripper columns. Figure 11 shows a weak correlation between CO_2 concentration and steam pressure. The CO_2 concentration of the rich absorbent in ABS2 decreases as the steam pressure increases. Due to the exothermic nature of the absorption reaction, higher temperatures in the absorber reduce the CO_2 absorption capacity of MEA. Thus, increased steam pressure will reduce the

CO_2 concentration of the rich absorbent in the absorber column. On the other hand, increasing steam pressure leads to higher temperatures in the stripper column and greater CO_2 removal % (Figure 12), indicating enhancement of CO_2 absorption. However, higher steam pressure results in larger reboiler heat requirements as demonstrated by Table 5.

Figure 13 illustrates the influence of steam pressure on the individual energy components of reboiler heat duty. Similar to flue gas and absorbent flow rate, $Q_{desorption}$ remains constant at 1.9 MJ/kg CO_2 across the range of steam pressures. As steam pressure increases, there is a reduction in $Q_{sensible}$ due to the decrease in temperature difference between absorbent exiting and entering the stripper column. As shown in Figure 13, $Q_{condenser}$ has a dominant effect on reboiler heat duty as steam pressure varies. As steam pressure rises, $Q_{condenser}$ significantly increases due to greater cooling requirements.

3.4 Overall Effect of Flexible Operation

3.4.1 Response Time

The response time for each process parameter at each column has been presented in Table 6. The response of changing a process parameter can be observed as (i) time for the system to reach the set-point value, (ii) time when temperature begins to change, (iii) time to reach steady state, and (iv) time when CO_2 removal % begins to change. Flow control loops are recognised as having the fastest dynamics and response times (Smith, 2002). This study demonstrates that the dynamics of the liquid absorbent flow is slower compared to flue gas flow. As Table 6 demonstrates, there is a greater lag time for the process to reach the set-point absorbent flow rate compared to flue gas flow and steam pressure. The CO_2 removal % has the slowest response time to steam pressure disturbances but responds relatively rapidly to changes in absorbent flow rate and flue gas flow rate.

The response time to a change in a process parameter differs in each of the plant columns due to the sequence of the columns in the pilot plant. Table 6 shows that a disturbance in flue gas flow rate, initiates a temperature change in ABS2 before ABS1 and stripper column. The initial effect of a disturbance in flue gas flow rate is observed in ABS2 since the feed gas enters this column first. On the other hand, modifying the absorbent flow rate will initiate a temperature change in ABS1 since the feed absorbent enters this column first. Lastly, initial response from altering the steam pressure primarily affects the stripper. After 20 to 30 minutes, a change in temperature will be observed in ABS2 and ABS1. Upon altering one of the process

parameters, a temperature response will occur within minutes, however the pilot plant requires over one hour to reach steady state.

Table 6: Response time (in minutes) to changes in process parameters for Absorber Column 2, Absorber Column 1 and stripper column in the CSIRO PCC pilot plant.

Process Parameter	Time to reach set-point	Time of observed change in CO_2 removal %	Absorber Column 2 (ABS2)		Absorber Column 1 (ABS1)		Stripper Column (STR)	
			Time temperature change observed	Time to reach steady state	Time temperature change observed	Time to reach steady state	Time temperature change observed	Time to reach steady state
Flue gas flow	4.8	1.0	1.0	74.3	2.3	85.3	3.3	88.3
Absorbent flow	6.5	3.0	1.5	92.7	1.0	90.7	2.8	99.8
Steam pressure	4.5	31.0	34.2	76.5	20.3	72.3	1.0	46.2

3.4.2 CO_2 Absorption and Energy Requirements

The temperature profiles in Figures 2, 5 and 10 illustrate the effect of changing process parameters on column performance (once steady state is reached). Flue gas flow rate, absorbent flow rate and steam pressure directly influence CO_2 absorption reaction (exothermic) which will affect temperature. Additionally, the temperature inside the columns is influenced by the temperature differences between the flue gas and liquid absorbent feed streams. The steam pressure parameter adjusts the temperature inside all of the columns. Hence, the step-changes to flue gas flow, absorbent flow and steam pressure were detected as changes to the temperature profile (e.g. upward/downward temperature shifts or shape alterations).

Step-changes of flue gas flow rate, absorbent flow rate and steam pressure each have varied effect on the absorption and desorption sections of the PCC process. The residual CO_2 concentration of the lean absorbent exiting the stripper remains constant during step-changes; where the CO_2 concentration during changes in flue gas flow and absorbent flow is 6.2 % (w/w) and 4.8 % (w/w) respectively. In the absorption section, the change in CO_2 concentration across the range of step-changes varies with different parameters. During step-changes, the CO_2 concentration of rich absorbent (at density meter D3) has a minimum and maximum range of: (i) 10.4-10.9 % (w/w) for steam pressure, (ii) 10.1-11.0 (w/w) for absorbent flow rate, and (iii) 8.9-11.2 % (w/w) for flue gas flow rate. Compared to flue gas flow rate step-changes, there is a reduced minimum-maximum L/G range for absorbent flow rate step-changes (refer to Table 3 and Table 4). Hence, the CO_2 concentration range is smaller during step-changes to absorbent flow compared to flue gas flow.

The results for CO_2 removal % and reboiler heat duty can indicate the overall performance of the PCC process. Overall, the greatest CO_2 removal of 98% was observed during: (i) the lowest step-change for flue gas flow rate (60 kg/h), and (ii) the highest step-change for absorbent flow rate (8.0 L/min). The heat capacity for liquid is greater than gas. Subsequently, the reboiler heat duty on a MJ/h basis was greater at high absorbent flow rate 8.0 L/min (98.0 MJ/h) compared to low flue gas flow 60 kg/h (82.2 MJ/h). However, the high absorbent flow of 8.0 L/min produced 18.37 kg CO_2/h whereas low flue gas flow of 60 kg/h only produced 9.82 kg CO_2/h. Thus, the energy requirements on a MJ/kg CO_2 basis are significantly greater for flue gas flow of 60 kg/h (7.8MJ/kg CO_2) compared to absorbent flow 8 L/min (5.4 MJ/kg CO_2). Hence, using absorbent step-changes to adjust CO_2 removal % would provide considerable energy savings on a MJ/kg CO_2 basis.

Greater steam pressures achieved higher CO_2 removal (Table 5). However, there is a compromise between absorber and stripper performance during step-changes to steam pressure. For instance, higher steam pressures may improve CO_2 stripping; however the subsequent increases to absorber temperature would reduce the absorbent's capacity for CO_2 absorption. Conversely, reducing the steam pressure would reduce temperatures and enhance CO_2 absorption but reduce stripping capabilities. Further modelling work would reveal optimal steam pressures which provide the most efficient CO_2 absorption and stripping capabilities.

3.4.3 Column Coupling and Liquid Distribution

Uniform liquid distribution of the absorbent is essential to maintaining expected packed column performance (Rukovena and Cai, 2008). The effectiveness of liquid distribution depends on: (i) approach to column coupling, and (ii) installation of liquid distributors and redistributor plates in the columns. Some key features in PCC plants that will influence the way columns are coupled include:

- piping configuration;
- number of columns;
- connectivity of columns – series or parallel;
- heat transfer on intermediate streams (heat exchangers, insulation, material of construction, pipe diameter and length);

Column coupling varies from one PCC plant to another. Thus, it is important to consider column coupling before making comparisons between experimental results from different pilot plant studies. Also, the accuracy of process models can be improved by accounting for column coupling effects. For instance, a

process model of the dual absorbers from this study should consider that the inter-cooler between the columns and that each column differs in absorption performance.

The online measurement of CO_2 removal % provides instantaneous insight into the performance of the absorption process. Even after the set-point of a parameter is reached in Figures 4, 7 and 12, there is still some variance in CO_2 removal %. This variability indicates that the liquid distribution of the system is still stabilising. As the distribution of liquid stabilises, the CO_2 loading of the lean and rich absorbent will reach a new steady state level. The time required to stabilise liquid distribution varies with different parameter changes. Absorbent flow rate changes generally requires more time for liquid redistribution compared to flue gas flow. Hence, as the system establishes a steady state, greater variance in CO_2 removal % is observed during absorbent step-changes (Figure 7) compared to flue gas step-changes (Figure 4).

For each absorber, there is a liquid redistribution plate in the middle the packing. These plates gather the liquid at the column walls to redistribute it over the packing evenly. In the case of flexible operation, these redistribution plates can significantly improve the stabilisation time for liquid distribution. They also will reduce the noise of measurements inside the columns. Understanding liquid distribution and column coupling has provided invaluable insight into the column dynamics of the PCC process.

4. Conclusion and Further Work

Practical experience in flexible operation of PCC pilot plants will be essential for the development of accurate dynamic models. Collecting dynamic data from a pilot plant is challenging as transient behaviour can be highly variable and difficult to reproduce. This study demonstrates the successful implementation of flexible operation in the form of parameter step-changes to a PCC process. The operation of the PCC plant under a broad range of transient conditions has captured the dynamics of the process and provides suitable data dynamic model validation. It is important to highlight that the dynamic behaviour and response times observed during this study is specific for this particular pilot plant. Although PCC plants of different scales would have different response times, it is likely the dynamic trends to parameter changes would be similar. Based on this study, changing the flue gas flow rate would produce the most rapid response. The greatest CO_2 removal % was achieved at the lowest flue gas flow rate or at the highest absorbent flow rate. However, the latter provides high CO_2 removal % with improved energy efficiency (significantly lower reboiler heat duty in terms of MJ/kg CO_2). The steam pressure parameter provides the ability to adjust the temperature of all

the columns simultaneously. This may be used to compensate for effects from ambient conditions or heat losses.

Planned future work for this study will include the validation of an Aspen Plus Dynamics PCC® model against this dynamic pilot plant data. Also, flexible PCC operation will be modelled to identify and optimise key process parameters that influence plant performance. Dynamic pilot plant studies such as this one will be important for the optimisation of further pilot plant experiments and accurate upscaling of industrial processes. Further pilot plant work will be fundamental to understanding the dynamic behaviour of a PCC plant. Recommended future flexible pilot plant studies should investigate:

- Comparison of dynamic operation in pilot plants of different configurations, scale or specifications (i.e. single absorber versus dual absorber, or structure packing);
- The influence of process step-changes on the shape of the temperature profile for each column, requires a sufficient number of temperature measurement along the packed bed;
- The effect of step-changing other process parameters (e.g. CO_2 concentration in the flue gas feed, MEA concentration);
- The impact of absorbent degradation on the performance of the PCC process during dynamic operation;
- The impact of different process control strategies during dynamic operation;
- The effect of column coupling and liquid distribution on the process dynamics.

Acknowledgements

Appendix A. Error Quantification

The absolute error for the online measurements from the temperature detectors is 1 °C. The absolute error for the other pilot plant instrumentation and the systematic error for gas analyser equipment can be found in

Artanto et al. (2012). The onsite MEA concentration measurements during pilot plant operation are based on triplicate titrations. The error for CO_2 removal % (based on gas analysis) varies between 5 to 6%. The standard errors for liquid analysis measurements (e.g. CO_2 and amine concentration, CO_2 loading, density) are based on duplicate determinations. According to the Endress & Hauser product specifications, the density meters have a measured error of ±1.2% and non-repeatability (reproducibility) within ±0.002 g/cm^3. The absolute measured error for the density meters was observed within the range of 0.16% to 0.86% with reasonable reproducibility (lower than product specifications). The error for reboiler heat duty varies within 0.2 and 0.4 MJ/kg CO_2.

B. 1. Experimental results for step-changes in flue gas flow rate. The operating set point conditions are absorbent flow rate of 5.5 L/min and steam pressure 140 kPag. Note z is the packed bed height from the bottom.

Flue gas flow rate	60 kg/h 26/10/12	80 kg/h 26/10/12	90 kg/h 29/10/12	100 kg/h 26/10/12	120 kg/h 26/10/12	120 kg/h 23/10/12
L/G ratio	7.09	5.32	4.73	4.26	3.55	3.55
Ambient Temp (°C)	15.1	15.3	25.8	14.9	16.9	25.6
CO_2 Removal %	98	95	92	87	82	80
Reboiler Heat Duty (MJ/kg CO_2)	7.8	7.0	6.3	5.9	5.5	5.8
MEA Concentration (wt %)	29.8	29.8	29.7	29.8	29.8	29.2
Mass Fraction of CO_2 Exit of ABS2	0.0910	0.0989	0.1017	0.1040	0.1102	0.1108
Mass Fraction of CO_2 Exit of Stripper	0.0641	0.0602	0.0599	0.0627	0.0636	0.0651
CO_2 Outlet Flow (kg/h)	9.82	14.24	15.52	15.36	17.57	17.18
ABS2						
Temperature (°C)						
z = 0.00 m	57.60	57.01	55.42	49.32	45.55	48.67
z = 1.35 m	53.31	63.14	62.46	58.57	53.97	56.51
z = 2.70 m	44.08	55.72	59.45	52.87	49.94	56.11
Bottom Pressure (kPa)	104.87	104.63	105.34	106.13	107.45	107.07
Pressure Drop (kPa)	1.35	1.27	1.07	1.19	1.73	1.25
ABS1						
Temperature (°C)						
z = 0.00 m	45.66	57.21	62.88	56.30	54.85	60.10
z = 1.35 m	44.22	56.63	69.51	65.71	65.21	68.38
z = 2.70 m	24.20	25.69	33.68	28.88	32.64	40.83
Bottom Pressure (kPa)	103.01	103.12	103.05	103.34	104.18	103.55
Pressure Drop (kPa)	2.25	2.00	2.34	3.27	3.68	3.49
Stripper						
Temperature (°C)						
z = 0.98 m	114.42	113.13	113.41	112.67	112.88	113.73
z = 1.98 m	112.70	110.98	110.91	109.47	110.09	111.52
z = 2.93 m	111.34	107.63	104.84	103.72	106.74	106.29
z = 3.90 m	110.99	108.05	106.49	104.22	104.19	105.92
Bottom Pressure (kPa)	159.00	151.86	151.77	151.82	153.40	151.90
Pressure Drop (kPa)	0.21	0.31	0.66	0.30	0.47	0.76

Absorbent flow rate	5.5 L/min 12/11/12	6.0 L/min 12/11/12	6.5 L/min 12/11/12	7.0 L/min 12/11/12	7.5 L/min 12/11/12	8.0 L/min 16/11/12
L/G ratio	4.26	4.65	5.03	5.42	5.81	6.19
Ambient Temp (°C)	20.9	22.90	25.6	30.1	29.5	20.2
CO_2 Removal %	83	86	92	94	98	98
Reboiler Heat Duty (MJ/kg CO_2)	5.8	5.9	5.9	5.7	5.5	5.4
MEA Concentration (wt %)	30.3	30.3	30.3	30.3	30.3	30.6
Mass Fraction of CO_2 Exit of ABS2	0.0890	0.0867	0.0848	0.0841	0.0834	0.0823
Mass Fraction of CO_2 Exit of Stripper	0.0457	0.0449	0.0455	0.0458	0.0469	0.0477
CO_2 Outlet Flow (kg/h)	15.77	16.60	16.85	17.66	18.04	18.37
ABS2						
Temperature (°C)						
z = 0.00 m	49.74	52.82	56.00	57.31	58.80	59.23
z = 1.35 m	56.54	60.25	63.56	65.29	66.59	67.10
z = 2.70 m	51.78	55.70	60.00	65.42	66.62	62.97
Bottom Pressure (kPa)	105.18	105.69	106.62	107.67	109.44	112.36
Pressure Drop (kPa)	0.96	1.03	1.32	1.62	2.54	4.21
ABS1						
Temperature (°C)						
z = 0.00 m	58.18	59.37	63.54	66.22	59.97	51.65
z = 1.35 m	65.90	67.27	67.75	64.72	51.93	44.03
z = 2.70 m	33.74	34.30	33.06	33.81	33.25	27.86
Bottom Pressure (kPa)	103.20	103.23	103.48	103.71	104.68	106.31
Pressure Drop (kPa)	2.26	2.66	3.18	3.85	4.62	5.14
Stripper						
Temperature (°C)						
z = 0.98 m	112.61	112.74	113.20	113.36	113.21	112.40
z = 1.98 m	108.82	109.31	109.90	110.36	109.73	107.94
z = 2.93 m	102.76	102.10	102.74	104.20	103.45	101.02
z = 3.90 m	103.53	103.96	104.77	104.23	103.69	100.25
Bottom Pressure (kPa)	151.80	151.75	151.66	152.11	153.61	153.72
Pressure Drop (kPa)	0.43	0.60	0.82	1.65	2.76	3.08

Steam Pressure	120 kPag 14/11/12	140 kPag 12/11/12	160 kPag 20/11/12	161 kPag 20/11/12	165 kPag 20/11/12
L/G ratio	4.26	4.26	4.26	4.26	4.26
Ambient Temp (°C)	18.9	20.9	21.3	23.2	26.8
CO_2 Removal %	71	80	89	92	93
Reboiler Heat Duty (MJ/kg CO_2)	5.3	5.8	6.6	7.2	7.4
MEA Concentration (wt %)	30.0	30.3	30.6	30.6	30.6
Mass Fraction of CO_2 Exit of ABS2	0.0830	0.0890	0.0927	0.0917	0.0930
Mass Fraction of CO_2 Exit of Stripper	0.0431	0.0457	0.0459	0.0482	0.0457
CO_2 Outlet Flow (kg/h)	14.45	15.77	17.15	15.97	17.44
ABS2					
Temperature (°C)					
z = 0.00 m	47.13	49.74	52.59	53.49	54.41
z = 1.35 m	53.47	56.54	61.31	62.28	62.64
z = 2.70 m	47.89	51.78	57.17	57.94	59.52
Bottom Pressure (kPa)	106.01	105.18	105.91	106.15	106.00
Pressure Drop (kPa)	1.24	0.96	0.92	0.94	0.91
ABS1					
Temperature (°C)					
z = 0.00 m	52.79	58.18	61.26	60.47	62.82
z = 1.35 m	64.72	65.90	69.07	68.72	69.72
z = 2.70 m	32.53	33.74	36.41	36.39	38.73
Bottom Pressure (kPa)	103.47	103.20	103.21	103.12	103.08
Pressure Drop (kPa)	2.88	2.26	2.76	3.00	2.98
Stripper					
Temperature (°C)					
z = 0.98 m	110.54	112.61	114.48	114.82	115.16
z = 1.98 m	105.51	108.82	112.40	113.12	113.74
z = 2.93 m	101.10	102.76	105.97	107.40	111.66
z = 3.90 m	99.04	103.53	107.66	109.04	108.23
Bottom Pressure (kPa)	150.28	151.80	152.52	152.94	153.28
Pressure Drop (kPa)	0.28	0.43	0.83	0.94	1.37

Appendix C. Effect of Ambient Temperature on Column Profiles
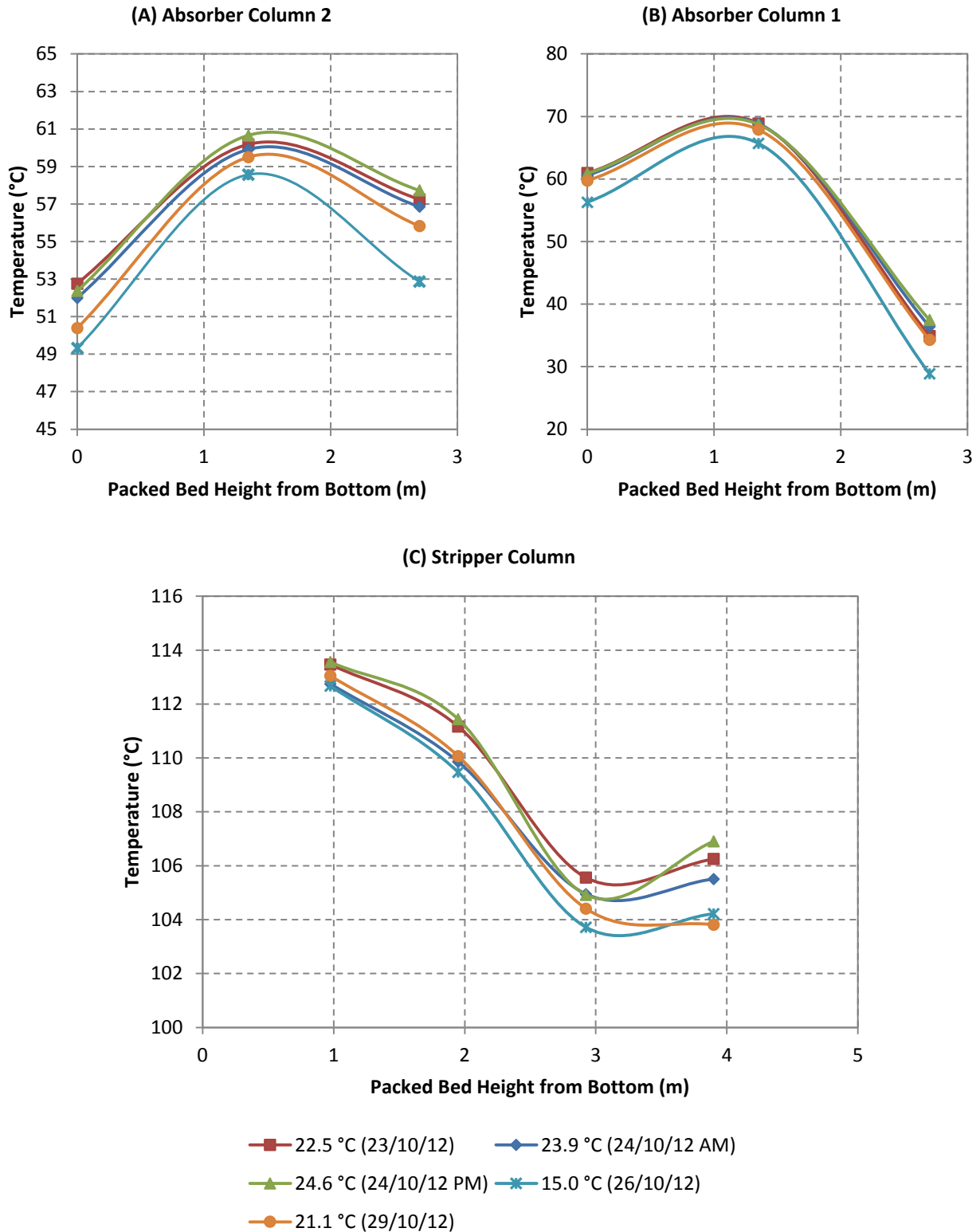
(A) Absorber Column 2

(B) Absorber Column 1

(C) Stripper Column

C. 1. Column temperature profiles for (A) Absorber Column 2, (B) Absorber Column 1, and (C) Stripper Column for runs of the same operating set-point conditions but different ambient temperature. The set point conditions are flue gas flow rate of 100 kg/h, absorbent flow rate of 5.5 L/min and steam pressure 140 kPag.

References

Arce, A., Mac Dowell, N., Shah, N. & Vega, L. F. (2012). Flexible operation of solvent regeneration systems for CO_2 capture processes using advanced control techniques: Towards operational cost minimisation. *International Journal of Greenhouse Gas Control,* 11**,** 236–250.

Artanto, Y., Attalla, M. I., Cottrell, A., Jansen, J., McGregor, J. M., Meuleman, E. E. B., Morgan, S., Osborn, M., Pearson, P., Wardhaugh, L. & Feron, P. H. M. (2009). A preliminary evaluation of post-combustion CO_2 capture performance in a pilot plant test using mono-ethanolamine at a lignite-fuelled power station in Australia. Fourth International Conference of Clean Coal Technologies for our Future (CCT2009), Dresden, Germany.

Artanto, Y., Jansen, J., Pearson, P., Do, T., Cottrell, A., Meuleman, E. & Feron, P. (2012). Performance of MEA and amine-blends in the CSIRO PCC pilot plant at Loy Yang Power in Australia. *Fuel,* 101**,** 264–275.

Artanto, Y., Jansen, J., Pearson, P., Puxty, G., Cottrell, A., Meuleman, E. & Feron, P. (2014). Pilot-scale evaluation of AMP/PZ to capture CO_2 from flue gas of an Australian brown coal–fired power station. *International Journal of Greenhouse Gas Control,* 20**,** 189–195.

Biliyok, C., Lawal, A., Wang, M. & Seibert, F. (2012). Dynamic modelling, validation and analysis of post-combustion chemical absorption CO_2 capture plant. *International Journal of Greenhouse Gas Control,* 9**,** 428–445.

Bui, M., Gunawan, I., Verheyen, T. V., Meuleman, E. & Feron, P. (2014a). Dynamic operation of post-combustion CO_2 capture in Australian coal-fired power plants. 12th International Conference on Greenhouse Gas Control Technologies (GHGT-12), Austin, Texas, USA. *Energy Procedia*, 63**,** 1368–1375.

Bui, M., Gunawan, I., Verheyen, V., Feron, P., Meuleman, E. & Adeloju, S. (2014b). Dynamic modelling and optimisation of flexible operation in post-combustion CO_2 capture plants—A review. *Computers & Chemical Engineering,* 61**,** 245–265.

Chen, Q., Kang, C., Xia, Q. & Kirschen, D. S. (2012). Optimal flexible operation of a CO_2 capture power plant in a combined energy and carbon emission market. *IEEE Transactions on Power Systems,* 27 (3)**,** 1602–1609.

Cohen, S. M., Rochelle, G. T. & Webber, M. E. (2010a). Optimal operation of flexible post-combustion CO_2 capture in response to volatile electricity prices. 10th International Conference on Greenhouse Gas Control Technologies (GHGT-10), Amsterdam, Netherlands. *Energy Procedia*, 4**,** 2604–2611 (2011).

Cohen, S. M., Rochelle, G. T. & Webber, M. E. (2010b). Turning CO_2 capture on and off in response to electric grid demand: A baseline analysis of emissions and economics. *Journal of Energy Resources Technology,* 132 (2)**,** 021003-1–021003-8.

Cohen, S. M., Webber, M. E. & Rochelle, G. T. (2012). The impact of electricity market conditions on the value of flexible CO_2 capture. Proceedings from ASME International Mechanical Engineering Congress and Exposition (IMECE), Texas, United States. *The American Society of Mechanical Engineers (ASME)*, 6**,** 581–593.

Cottrell, A. J., McGregor, J. M., Jansen, J., Artanto, Y., Dave, N., Morgan, S., Pearson, P., Attalla, M. I., Wardhaugh, L., Yu, H., Allport, A. & Feron, P. H. M. (2008). Post-combustion capture R&D and pilot plant operation in Australia. 9th International Conference on Greenhouse Gas Control Technologies (GHGT-9), Washington DC, USA. *Energy Procedia*, 1**,** 1003–1010 (2009).

Cousins, A., Cottrell, A., Lawson, A., Huang, S. & Feron, P. H. M. (2012). Model verification and evaluation of the rich-split process modification at an Australian-based post combustion CO_2 capture pilot plant. *Greenhouse Gases: Science and Technology,* 2 (5)**,** 329–345.

Dave, N., Do, T., Palfreyman, D. & Feron, P. H. M. (2011). Impact of liquid absorption process development on the costs of post-combustion capture in Australian coal-fired power stations. *Chemical Engineering Research and Design,* 89 (9)**,** 1625–1638.

Dugas, R. E. (2006). *Pilot Plant Study of Carbon Dioxide Capture by Aqueous Monoethanolamine.* Masters Thesis, The University of Texas at Austin.

Faber, R., Köpcke, M., Biede, O., Knudsen, J. N. & Andersen, J. (2010). Open-loop step responses for the MEA post-combustion capture process: Experimental results from the Esbjerg pilot plant. 10th International Conference on Greenhouse Gas Control Technologies (GHGT-10), Amsterdam, The Netherlands. *Energy Procedia*, 4**,** 1427–1434 (2011).

Gayheart, J. W., Moorman, S. A., Parsons, T. R., Poling, C. W., Guan, X. & Wheeldon, J. M. (2012). Technical Paper: B&W PGG's RSAT^{TM} process and field demonstration of the OptiCap® advanced solvent at the US-DOE's National Carbon Capture Center. Power Plant Air Pollutant Control "MEGA" Symposium, Baltimore, Maryland, USA. *Babcock & Wilcox Power Generation Group***,** 1–9.

Gruber, G. (2004). Dynamic Model of a Scrubber Using Aspen Plus. Aspen World 2004, Orlando, Florida, USA. *Merck & Co., Inc.*

Husebye, J., Anantharaman, R. & Fleten, S.-E. (2011). Techno-economic assessment of flexible solvent regeneration & storage for base load coal-fired power generation with post combustion CO_2 capture. *Energy Procedia,* 4**,** 2612–2619.

IPCC (2014). Climate Change 2014: Synthesis Report of the Fifth Assessment Report of the Intergovernmental Panel on Climate Change. Core Writing Team, Pachauri, R. K., Meyer, L. (Editors). Geneva, Switzerland: *Intergovernmental Panel on Climate Change (IPCC)*.

Islam, M. S., Yusoff, R., Ali, B. S., Islam, M. N. & Chakrabarti, M. H. (2011). Degradation studies of amines and alkanolamines during sour gas treatment process. *International Journal of Physical Sciences,* 6 (25)**,** 5877–5890.

Kvamsdal, H. M., Chikukwa, A., Hillestad, M., Zakeri, A. & Einbu, A. (2010). A comparison of different parameter correlation models and the validation of an MEA-based absorber model. 10th International Conference on Greenhouse Gas Control Technologies (GHGT-10), Amsterdam, Netherlands. *Energy Procedia*, 4**,** 1526–1533 (2011).

Kvamsdal, H. M., Jakobsen, J. P. & Hoff, K. A. (2009). Dynamic modeling and simulation of a CO_2 absorber column for post-combustion CO_2 capture. *Chemical Engineering and Processing: Process Intensification,* 48 (1)**,** 135–144.

Lawal, A., Wang, M., Stephenson, P., Koumpouras, G. & Yeung, H. (2010). Dynamic modelling and analysis of post-combustion CO_2 chemical absorption process for coal-fired power plants. *Fuel,* 89 (10)**,** 2791–2801.

Lawal, A., Wang, M., Stephenson, P. & Obi, O. (2012). Demonstrating full-scale post-combustion CO_2 capture for coal-fired power plants through dynamic modelling and simulation. *Fuel,* 101**,** 115–128.

Lawal, A., Wang, M., Stephenson, P. & Yeung, H. (2009a). Dynamic modeling and simulation of CO_2 chemical absorption process for coal-fired power plants. 10th International Symposium on Process Systems Engineering-PSE2009, Brazil. *Computer Aided Chemical Engineering*, 27**,** 1725–1730.

Lawal, A., Wang, M., Stephenson, P. & Yeung, H. (2009b). Dynamic modelling of CO_2 absorption for post combustion capture in coal-fired power plants. *Fuel,* 88 (12)**,** 2455–2462.

Lepaumier, H., Picq, D. & Carrette, P. L. (2008). Degradation study of new solvents for CO_2 capture in post-combustion. 9th International Conference on Greenhouse Gas Control, Washington DC, USA. *Energy Procedia*, 1**,** 893–900 (2009).

Lin, Y.-J., Wong, D. S.-H., Jang, S.-S. & Ou, J.-J. (2012). Control strategies for flexible operation of power plant with CO_2 capture plant. *AIChE Journal,* 58 (9)**,** 2697–2704.

Mac Dowell, N. & Shah, N. (2013). Identification of the cost-optimal degree of CO_2 capture: An optimisation study using dynamic process models. *International Journal of Greenhouse Gas Control,* 13**,** 44–58.

Mac Dowell, N. & Shah, N. (2015). The multi-period optimisation of an amine-based CO_2 capture process integrated with a super-critical coal-fired power station for flexible operation. *Computers & Chemical Engineering,* 74**,** 169–183.

Moser, P., Schmidt, S., Sieder, G., Garcia, H. & Stoffregen, T. (2011). Performance of MEA in a long-term test at the post-combustion capture pilot plant in Niederaussem. *International Journal of Greenhouse Gas Control,* 5 (4)**,** 620–627.

Nittaya, T., Douglas, P. L., Croiset, E. & Ricardez-Sandoval, L. A. (2014). Dynamic modeling and evaluation of an industrial-scale CO_2 capture plant using monoethanolamine absorption processes. *Industrial & Engineering Chemistry Research,* 53 (28)**,** 11411–11426.

Rukovena, F. & Cai, T. (2008). Achieve good packed tower efficiency. *Chemical Processing,* 71 (11)**,** 22–31.

Seibert, F., Chen, E., Perry, M., Briggs, S., Montgomery, R. & Rochelle, G. (2010). UT/SRP CO_2 capture pilot plant — Operating experience and procedures. 10th International Conference on Greenhouse Gas Control Technologies, Amsterdam, The Netherlands. *Energy Procedia*, 4**,** 1616–1623 (2011).

Simon, L. L., Elias, Y., Puxty, G., Artanto, Y. & Hungerbuhler, K. (2011). Rate based modeling and validation of a carbon-dioxide pilot plant absorbtion column operating on monoethanolamine. *Chemical Engineering Research and Design,* 89 (9)**,** 1684–1692.

Smith, C. L. (2002). Intelligently tune PI controllers: automatic tuning offers only dubious advantages. (Instrumentation & Control). Chemical Engineering [Online]. Academic OneFile. Available: http://go.galegroup.com/ps/i.do?id=GALE%7CA91087854&v=2.1&u=monash&it=r&p=AONE&sw=w&asid=300d61c8d774ce7a4a8ef112a68d32dd [Accessed 24/07/2014].

Stéphenne, K. (2014). Start-up of world's first commercial post-combustion coal fired CCS project: Contribution of Shell Cansolv to SaskPower Boundary Dam ICCS Project. 12th International Conference on Greenhouse Gas Control Technologies (GHGT-12), Austin, Texas, United States. *Energy Procedia*, 63**,** 6106–6110.

van der Ham, L. V., Bakker, D. E., Geers, L. F. G. & Goetheer, E. L. V. (2014). Inline monitoring of CO_2 absorption processes using simple analytical techniques and multivariate modeling. *Chemical Engineering & Technology,* 37 (2)**,** 221–228.

van der Wijk, P. C., Brouwer, A. S., van den Broek, M., Slot, T., Stienstra, G., van der Veen, W. & Faaij, A. P. C. (2014). Benefits of coal-fired power generation with flexible CCS in a future northwest European power system with large scale wind power. *International Journal of Greenhouse Gas Control,* 28**,** 216–233.

van Eckeveld, A. C., van der Ham, L. V., Geers, L. F. G., van den Broeke, L. J. P., Boersma, B. J. & Goetheer, E. L. V. (2014). Online monitoring of the solvent and absorbed acid gas concentration in a CO_2 capture process using monoethanolamine. *Industrial & Engineering Chemistry Research,* 53 (13)**,** 5515–5523.

Zhang, Y., Ho, M. T. & Wiley, D. E. (2012). Investigating flexible carbon capture opportunities in the Australian electricity market. 11th International Conference on Greenhouse Gas Control Technologies (GHGT-11), Kyoto, Japan. *Energy Procedia*, 37**,** 2746–2753 (2013).

Figure Captions

Figure 1: Flow diagram of the CSIRO PCC pilot plant in the AGL Loy Yang power station, Victoria, Australia.

Figure 2: Temperature profiles for (A) Absorber Column 2, (B) Absorber Column 1, and (C) the Stripper Column revealing their temperature response due to step-changes in flue gas flow. The operating set point conditions are absorbent flow rate of 5.5 L/min and steam pressure 140 kPag.

Figure 3: Predicted CO_2 concentration for various flue gas flow rates at (A) density meter D3 and (B) density meter D2. The set point conditions as per Figure 2.

Figure 4: Change in CO_2 removal % (proportion of CO_2 absorbed from the feed flue gas) during step-changes to flue gas flow rate. The operating set point conditions as per Figure 2.

Figure 5: Column temperature profiles for (A) Absorber Column 2, (B) Absorber Column 1, and (C) Stripper Column showing step-change in absorbent flow. The operating set point conditions are flue gas flow rate of 100 kg/h and steam pressure 140 kPag.

Figure 6: Predicted CO_2 concentration for various absorbent flow rates at (A) density meter D3 and (B) density meter D2. The set point conditions are flue gas flow rate 100 kg/h and steam pressure 140 kPag.

Figure 7: Change in CO_2 removal (proportion of CO_2 absorbed from the feed flue gas) during step-changes to absorbent flow rate (proportion of CO_2 recovered from the feed flue gas as stripper CO_2 product). The set point conditions as per Figure 5.

Figure 8: Reboiler heat duty divided into the three components of desorption energy $Q_{desorption}$, $Q_{sensible}$ and $Q_{condenser}$ at various absorbent flow rates.

Figure 9: The correlation between steam pressure and reboiler temperature.

Figure 10: Column temperature profiles for (A) Absorber Column 2, (B) Absorber Column 1, and (C) Stripper Column showing step-change in steam pressure. The operating set point conditions are flue gas flow rate of 100 kg/h and absorbent flow rate of 5.5 L/min.

Figure 11: Predicted CO_2 concentration for various steam pressures at density meter D3. The set point conditions as per Figure10.

Figure 12: Change in CO_2 removal (proportion of CO_2 absorbed from the feed flue gas) during step-changes to steam pressure. The operating set point conditions as per Figure 10.

Figure 13: Reboiler heat duty divided into the three components of desorption energy $Q_{desorption}$, $Q_{sensible}$ and $Q_{condenser}$ at various steam pressures.

C. 1. Column temperature profiles for (A) Absorber Column 2, (B) Absorber Column 1, and (C) Stripper Column for runs of the same operating set-point conditions but different ambient temperature. The set point conditions are flue gas flow rate of 100 kg/h, absorbent flow rate of 5.5 L/min and steam pressure 140 kPag

Table Captions

Table 1: Typical brown coal flue gas composition from the AGL power station, adapted from Artanto et al. (2012).

Table 2: Parameter range for stable operation of the CSIRO pilot plant at Loy Yang Power and the actual operating range used for the dynamic step-change approach.

Table 3: Average CO_2 removal % (based on the gas analysis) and reboiler heat duty for different flue gas flow rates at the CSIRO PCC pilot plant. The set point conditions as per Figure 2.

Table 4: Average CO_2 removal % (based on the gas analysis) and reboiler heat duty for different absorbent flow rates. The set point conditions as per Figure 5.

Table 5: Average CO_2 removal (based on the gas analysis) and reboiler heat duty for different steam pressures at the CSIRO PCC pilot plant. The set point conditions as per Figure 10.

Table 6: Response time (in minutes) to changes in process parameters for Absorber Column 2, Absorber Column 1 and Stripper Column in the CSIRO PCC pilot plant.

B. 1. Experimental results for step-changes in flue gas flow rate. The operating set point conditions are absorbent flow rate of 5.5 L/min and steam pressure 140 kPag. Note z is the packed bed height from the bottom.

B. 2. Experimental results for step-changes in absorbent flow rate. The operating set point conditions are flue gas flow rate of 100 kg/h and steam pressure 140 kPag. Note z is the packed bed height from the bottom.

B. 3. Experimental results for step-changes in steam pressure. The operating set point conditions are flue gas flow rate of 100 kg/h and absorbent flow rate of 5.5 L/min. Note z is the packed bed height from the bottom.